AKADÉMIAI KIADÓ

UNIVERSITY of DEBRECEN

International Review of Applied Sciences and Engineering

14 (2023) 1, 13–24

DOI:
10.1556/1848.2022.00380

ORIGINAL RESEARCH PAPER

Design and analysis of grooved heat pipe

B. Kirubadurai[1*], K. Kanagaraja[2], G. Jegadeeswari[3] and T. Kumaran[1]

[1] Department of Aeronautical Engineering, Vel Tech Dr. Rangarajan Dr. Sagunthala R&D Institute of Science & Technology, Chennai, India

[2] Department of Mechanical Engineering, Rajalakshmi Institute of Technology, Chennai, India

[3] Department of Electrical and Electronics Engineering, AMET Deemed to be University, Chennai, India

Received: September 16, 2021 • Accepted: March 9, 2022
Published online: September 7, 2022

ABSTRACT

A heat pipe is a heat conduction program that utilizes both heat permeability and regime shift concepts to transport heat effectively between 2 different lines. A heat pipe is made up of a pipe or tube and a base fluid. In practice, the heat pipe is poured into a mould that is compatible with the cooling media. These devices have found uses in a variety of fields, including space apparatus, solar energy systems, electronic equipment, and air conditioning systems, due to their simplicity of design and ease of manufacture and maintenance. Thermal performance improvement being the major concern in our project we researched different techniques. The heating surface area has a direct impact on heat transfer. Therefore, we have focused on heat enhancement by introducing grooves. Alongside we also considered using different materials for the pipe. At the end of our research, we are going to produce groove structure models with different materials and analyze them using ANSYS software and propose the best structures with highest thermal efficiency for different applications of heat pipes. This is an attempt to increase heat transmission in response to various material and structural changes. Heat transmission is improved with grooved heat pipes as well as heat transmission various with different types materials used in heat pipe.

KEYWORDS

heat pipe, thermal conductivity, grooved pipe, porous medium

INTRODUCTION

A heat pipe is a tubular system that uses a metal tube to hold the liquid under pressure and is extremely efficient at transmitting heat. A heat pipe is a tubular system that is very efficient in transmitting heat, using a metal container that holds the liquid under pressure, and the inner layer of the tube is lined with a porous material that functions as a wick [1, 2, 5]. The idea is the same in a heat pipe, which is made up of several wicks. The liquid evaporates into a gas, which travels to the pipe's cooler before reverting to a liquid and passing through the wick. So, by just using TPCL length, we can see how to optimize the wick shape [3, 4, 9]. We can see how to optimize the filament form just by using the TPCL distance. We know that heat pipes are very efficient at transferring heat, so they are used to allow use of all the thermal superconductor property by allowing for a high heat transfer rate, which allows the device ideal for a more range of applications and industrial works [7, 10, 15]. The inclusion of heat pipes to a variety of temperature scales and applications is a direct indicator of the technology's ability. The implementation's economic analysis showed a net annual energy savings of 134 MWh, with a one-month operating payback period (Fig. 1) [6, 8, 11].

We are even aware of the thermal transfer limitations of the heat pipe. There are various constraints on heat pipes, such as the base fluid, the structure of the wick, the dimensions and the temperature at which it is operated. There are also capillary constraints that create

*Corresponding author.
E-mail: bkirubadurai@gmail.com

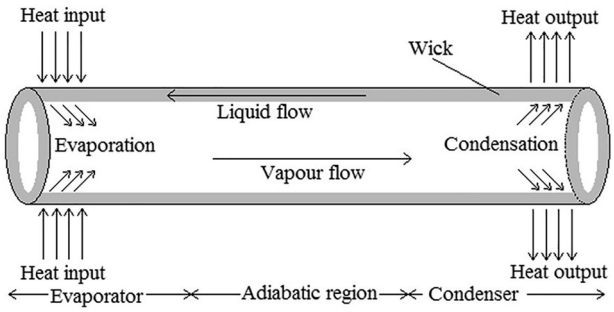

Fig. 1. Basic design of heat pipe

capillary distinctions around the liquid-vapour interfaces in the inlet and outlet [9, 11, 12]. Similarly, there are other limitations such as sonic limitation, limitation of entrainment, limitation of boiling, and heat pipe performance depends on the heat pipe groove width with grooved capillary structure [13, 14, 16]. All these limitations depend on the fluid properties of the thermos, the parameters of the wick and the heat pipe.

HEAT PIPE DESIGN

There are many factors to consider when building a heat pipe. Material properties, working limit, heat pipe length and diameter, power limitation, heat pipe transport limitation, thermal resistance, heat pipe bending and flattening effects, and operating orientation all receive significant attention [17, 18, 19] However, by specifying the types of copper/water, the design problems are reduced to a few key considerations. The amount of energy that the heat pipe will bear is perhaps the most major determinant [20, 21, 24, 26]. Another consideration is the temperature range under which the individual working fluid will function. To avoid contaminating the environment or causing a chemical reaction, this working fluid requires a compatible vessel content. Assume that both heat pipes are made of copper and have the same length and diameter of 60 and 3 mm, orderly. The formula is used to measure the rate of heat transfer [22, 23, 25, 26].

The conventional heat pipe: Here is an example of a general heat pipe with a sintered powder wick structure. The heat pipe is depicted in three dimensions below. The inner circle of the heat pipe has a diameter of 10 mm and a length of 200 mm (Fig. 2).

Grooved heat pipe: Using the concept of increasing the surface area, we introduced grooves over the inner walls of the pipe. This wick structure basically not only improves the capillary forces but also increases the surface area which results in increase of heat transfer and overall thermal efficiency of the heat pipe (Tables 1–3, Figs 3 and 4).

METHODOLOGY IN MATHEMATICS

Flow and heat transfer equations that govern flow and heat transmission

The volume of fluid (VOF) technique is utilised when there are particularly in non-source liquids. The stationary and non-stationary circumstances aspect of almost any gas/liquid operating is crucial when the operating liquids functionality is relevant. The scientific formula for the VOF model is similar.

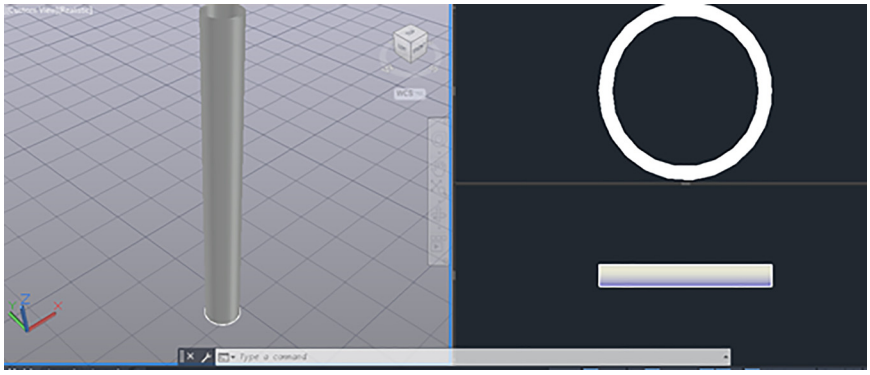

Fig. 2. Foundational heat pipe design

Table 1. Material operating temperature

Material	Operating temperature (K)		Operating temperature (°C)	
	Foundational	Grooved	Foundational	Grooved
Aluminum	284.35–366.20	284.41–414.74	11.2–93.05	11.26–41.59
Copper	283.29–374.37	282.41–421.12	10.14–101.22	9.26–147.97
Steel	296.86–313.24	295.02–336.19	23.71–40.09	21.87–63.04

Table 2. Properties of heat pipe

Location	Boundary	Momentum	Thermal
Insulated region	Wall	Shear state of a static wall – zero slide	Heat flux – 0
Cold region	Wall	Shear state of a static wall – zero slide	Constant temperature
Hot region	Wall	Shear state of a static wall – zero slide	Constant heat flux

Table 3. The numerical analysis parameters

Variable	Characterization
Kind of flow	Laminar
Duration	0.0001 s
Heat content	2455 kJ/kg
Temperature of saturation	373.15 K
Criteria of convergence	10^{-3} Pressure velocity
Association	Simple
Schemes of discretization	First order upwind

$$\frac{\partial}{\partial t}(\alpha_v \rho_v) + \nabla.\left(\alpha_v \rho_v \overrightarrow{u}_v\right) = S_M \tag{1}$$

$$\sum_{l=1}^{n} \alpha_1 = 1 \tag{2}$$

Equations of momentum (Navier-Stokes equations)

The mobility formulas in the amount of liquid method, as shown below, are focused on the quantity of densities and friction factor in term of phases weight fractions.

$$\frac{\partial}{\partial t}\left(\rho \overrightarrow{u}\right) + \nabla.\left(\rho \overrightarrow{u}\ \overrightarrow{u}\right) = -\nabla P + \rho \overrightarrow{g} + \nabla.\left[\mu\left(\nabla \overrightarrow{u} + \nabla \overrightarrow{u}^{T}\right)\right] + \overrightarrow{F} \tag{3}$$

$$\rho = \alpha_l \rho_l + \alpha_v \rho_v$$

$$\mu = \alpha_l \mu_l + \alpha_v \mu_v$$

where F is the outside force that acts on the coolants, g is gravity movement, and P is pressure.

To compensate for the surface tension effects of cryo-preservation, the uniformly distributed force (CSF) approach

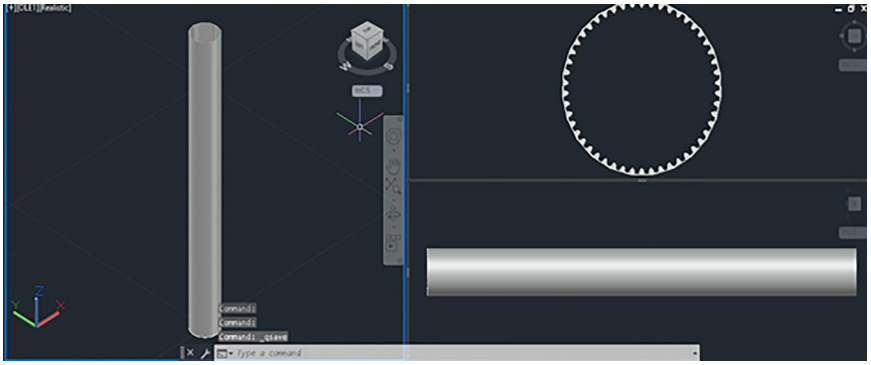

Fig. 3. Grooved heat pipe design

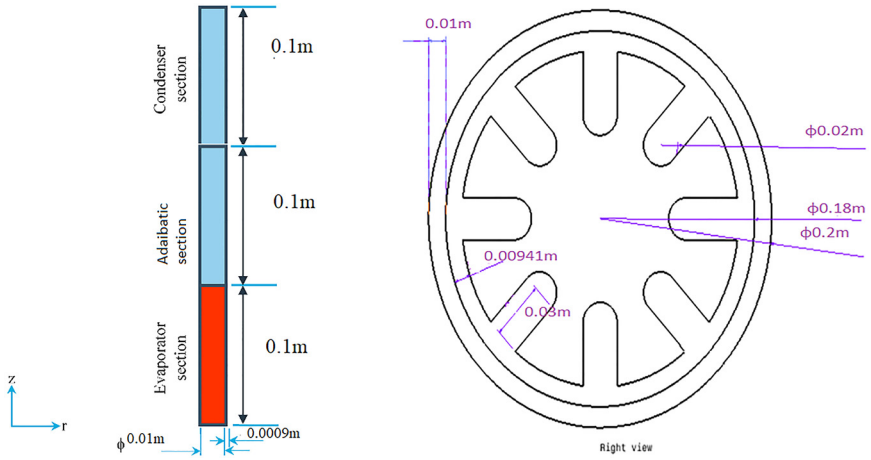

Fig. 4. Dimensions of heat pipe

is employed in combination with Black bill's mathematical model as follows:

$$Fcs = \sum_{pairsij,i<j} \frac{\sigma_{ij}(\alpha_i\rho_i C_i \nabla\alpha_i + \alpha_i\rho_j C_j \nabla\alpha_j)}{(\rho_i + \rho_j)/2} \quad (4)$$

The energy equation in volume of fluid (VOF) form is as follows:

The energy equation in (VOF)

$$\frac{\partial}{\partial t}(\rho C_p T) + \nabla.\left[\vec{u}(\rho C_p T + P)\right] = \nabla.(k\nabla T) + S_E \quad (5)$$

where SE denotes the energy equation's source term. Thermal conductivity, denoted by k, is computed as follows:

$$k = \alpha_l k_l + \alpha_v k_v \quad (6)$$

The mass-averaged variables, i.e., the energy term (E), are given by the equation below.

$$E = \frac{\alpha_l\rho_l E_l + \alpha_v\rho_v E_v}{\alpha_l\rho_l + \alpha_v\rho_v} \quad (7)$$

The mass-averaged variables, i.e. the energy term, are given by the following equation (E).

Boundary condition

The condenser portion has a constant wall temperature at thermal boundary conditions, whereas the evaporator has varying heat loads for each filling ratio. The wall motion is stationary in the momentum boundary condition (Fig. 5).

Meshing

ANSYS Meshing allows you to specify combinations of point elements, edge controls, surface controls, and/or body controls, giving you additional control. They each have their own set of choices and can be used to change the mesh in a variety of ways. Throughout this scenario, the automatic mesh form approach is applied, but the mesh sizing is done manually. The upper and lower mesh size restrictions are both set to 0.0002 m, as seen in the diagram below. When you use this control level, you will obtain a mesh with 61,1,65 nodes and 5,66,244 elements (Fig. 6).

Fluent solution setup

The procedures in this project include setting up the FLUENT solver and simulating the flow. Set up the solver by going to Materials > Selecting a solid and clicking Edit. Use the properties listed in Table 4 to make changes to the solid's properties.

RESULTS AND DISCUSSION

For each variant, various parameters such as density, temperature, and velocity were measured and compared. The effect of the evaporator, adiabatic wall, and condenser temperature are investigated in this simple heat pipe model with water as the heat exchanger and aluminum as the material (Table 5 and Fig. 7).

Conventional copper heat pipe has been analyzed and observed temperatures ranged with a minimum of 284.35 K and a maximum of 366.20 K. The effect of temperature in fluid zone, evaporator, adiabatic wall, and condenser is examined using with water as the heat transfer fluid and copper as the material. Conventional aluminum heat pipe has been analyzed and observed Temperatures ranged with a minimal of 282.41 K and a peak of 374.37 K. The result of temperature in fluid zone, evaporator, adiabatic wall, and condenser is examined using water as the cooling medium and steel as the material. Conventional steel heat pipe has been analyzed and observed in temperatures with a

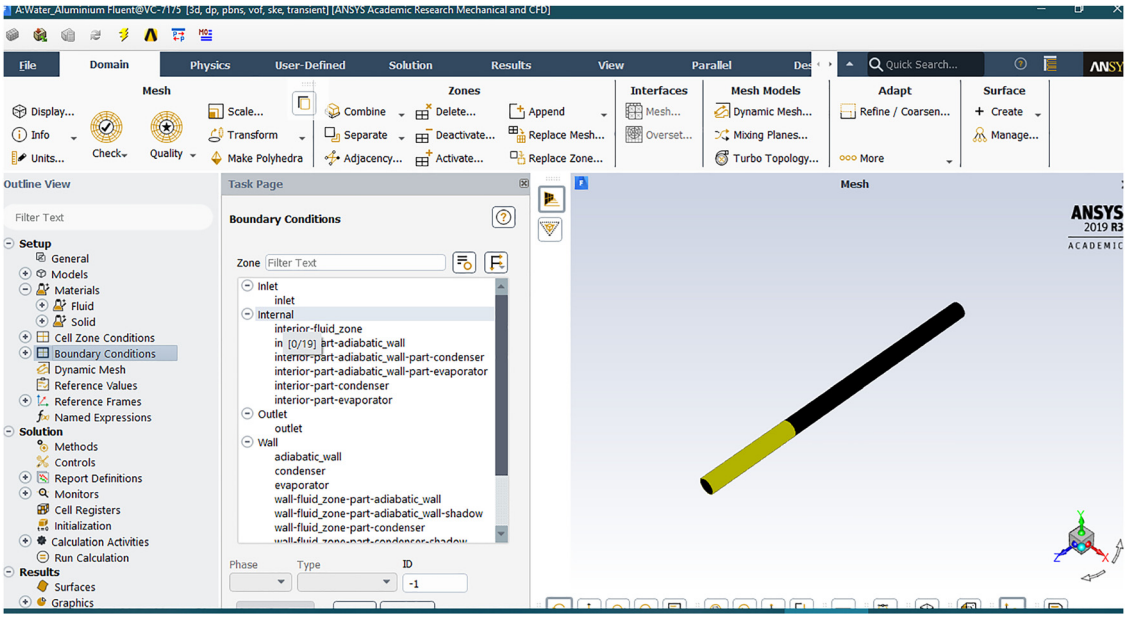

Fig. 5. Sequence of applying boundary condition

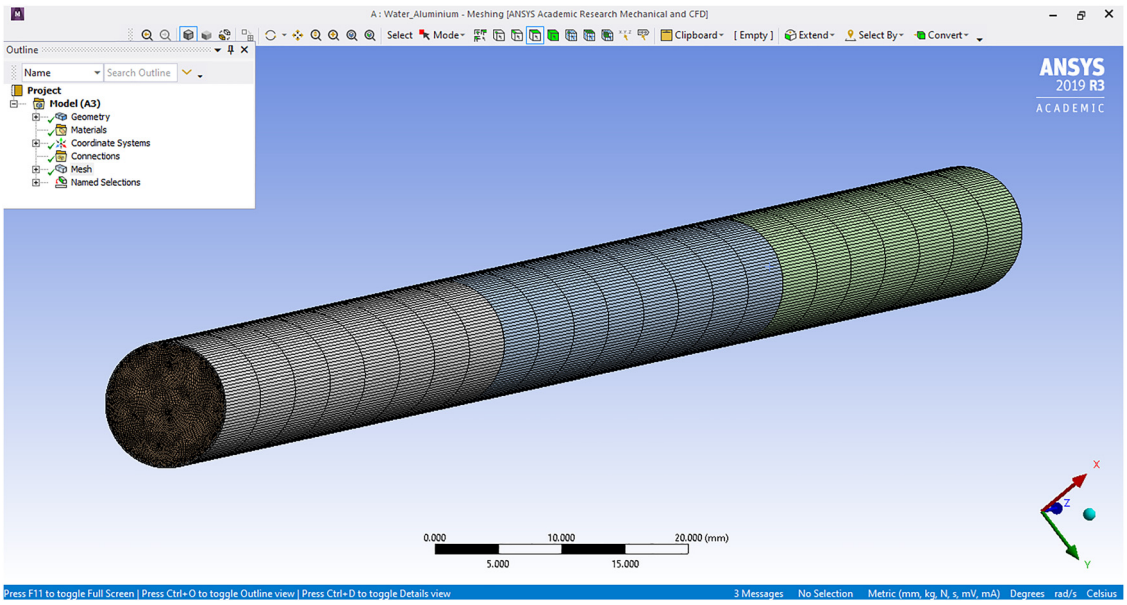

Fig. 6. Meshing of heat pipe

Table 4. Properties of solid material

Property	Aluminum	Steel	Copper
Density (kg m^{-3})	2,700	7,750–8,050	8,960
Thermal conductivity (W $(m^{-1}\cdot k^{-1})$	237	54	401
Boiling point	2,743	700–1800	2,835
Molar heat capacity J $(mol^{-1}\cdot k^{-1})$	24.2	0.466	24.44

Table 5. Properties of fluid

Point of boiling	100.00 °C
Limited density (at 3.98 °C)	1,000 kg m^{-3}
Density (25 °C)	99.701 kg m^{-3}
Pressure of vapour (25 °C)	23.75 Torr
Vaporization heat (100 °C)	40.65 KJ/mole
Vaporization entropy (25 °C)	118.8 J/°C mol
Viscosity	0.8903 Centipoise
Surface tension (25 °C)	0.7197 Dyn/meter

minimum of 296.86 K and a maximum of 313.24 K. The effect of temperature in fluid zone, evaporator, adiabatic wall, and condenser is examined using with water as the working fluid and steel as the material (Fig. 8).

Grooved copper heat pipe has been analyzed and observed in temperatures ranged with a minimum of 284.41 K and a maximum of 414.74 K. The effect of temperature in fluid zone, evaporator, adiabatic wall, and condenser is examined using water as the base fluid. Grooved aluminum heat pipe has been analyzed and observed in temperatures ranged with a minimum of 283.29 K and a maximum of 421.12 K. The effect of temperature in fluid zone, evaporator, adiabatic wall, and condenser is examined using water as the base fluid. Grooved copper heat pipe has been analyzed and observed in temperatures ranged with a minimum of 295.02 K and a maximum of 336.19 K. The effect of temperature in fluid zone, evaporator, adiabatic wall, and condenser is examined using water as the base fluid (Fig. 9).

Velocity influence in a heat pipe

A considerable extra heat is deposited on the bottom surface, which would be usually referred to as the liquid desiccant region. The simulation output for the vapour – phase pathway's evaporated portion is a red outline that turns bluish in the collection region. The speed applicable at the bottom vapour – phase path hugely puts more pressure of warm air at the drying segment, and heat was gradually diffused from the drying stage to the moderate frozen phase at the test section (green contour), and eventually to the coloured curves at the chiller segment. Later, as shown by the blue outline, the heat pipe's activity has caused the hot fluid to settle (Fig. 10).

Influence of pressure in heat pipe

The overall pressure contour demonstrates that the heat is spread equitably. Because of the green contour of the evaporation portion, the adiabatic section has a light blue contour, and the condensing section has a dark blue contour. The air particles smash smoothly because the container's surface area is greater than the vapour phase path. Even if the vapour path remains warm, the atmosphere at the container's interior surface is warm. Because the pressure is not dangerous, the structure does not break or fracture (Fig. 11, Tables 6 and 7).

Influence of temperature in heat pipe

Per the temperature profiles studies, the heat pipe finally implemented heated vapour to trapped moisture. This analysis

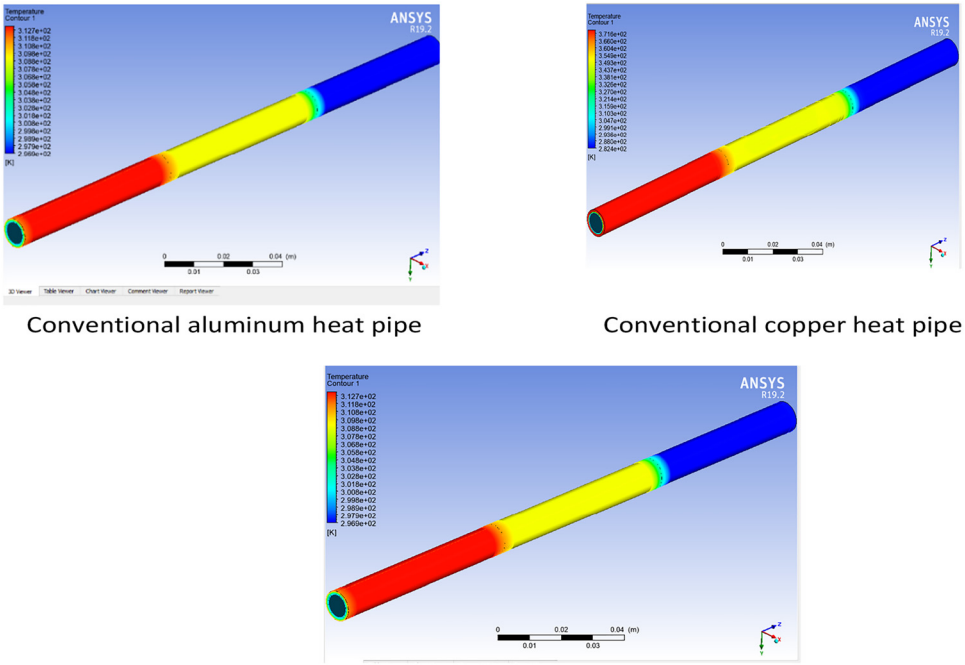

Fig. 7. Temperature distribution in conventional steel heat pipe

proved that somehow a narrow tube with an inherent wick arrangement enables for heating and cooling inside the tube, due to heat transference from the heating to the chilled side. As can be observed, the heat is symmetrical. It shows that the vapour stage has a conductivity, resulting in a high heat flux. The aldol condensation contracts energy in the regenerator, changing it to contracted gas, which would be then turned into a fluid. For its capacity to withstand extreme temps, copper has proven to be a good preference for pipe building projects.

Temperature data received at various axial intervals on the heat pipe core is used to construct axisymmetric heat flux. Figure shows the axial temperature field along the heat pipe during a dry run. The graphic depicts the temperature variations in the evaporator, adiabatic section, and

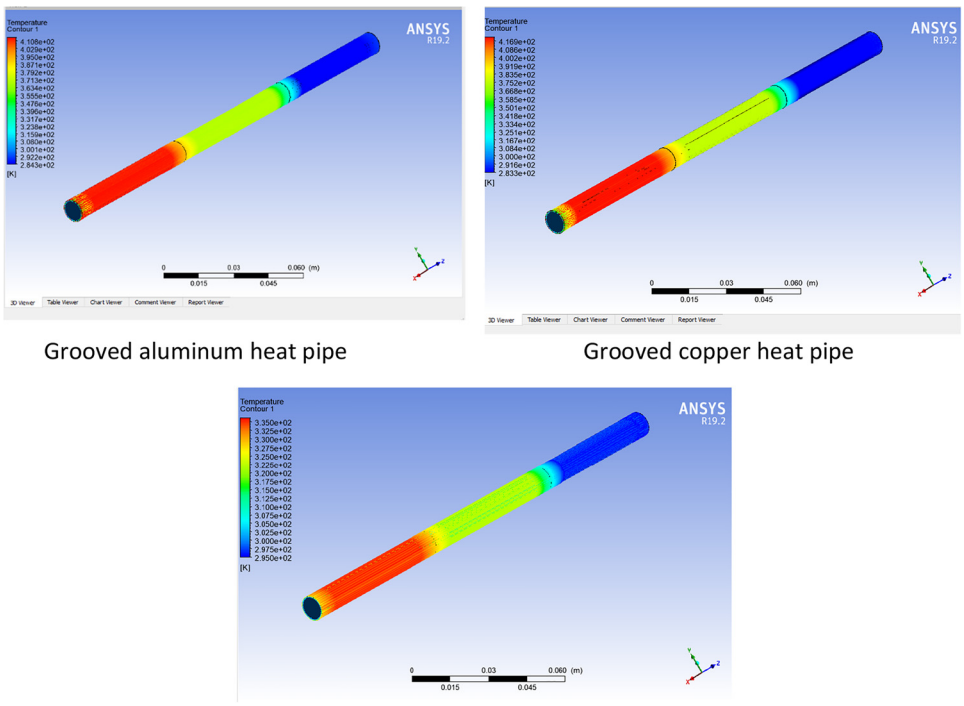

Fig. 8. Distribution of temperature in grooved steel heat pipe

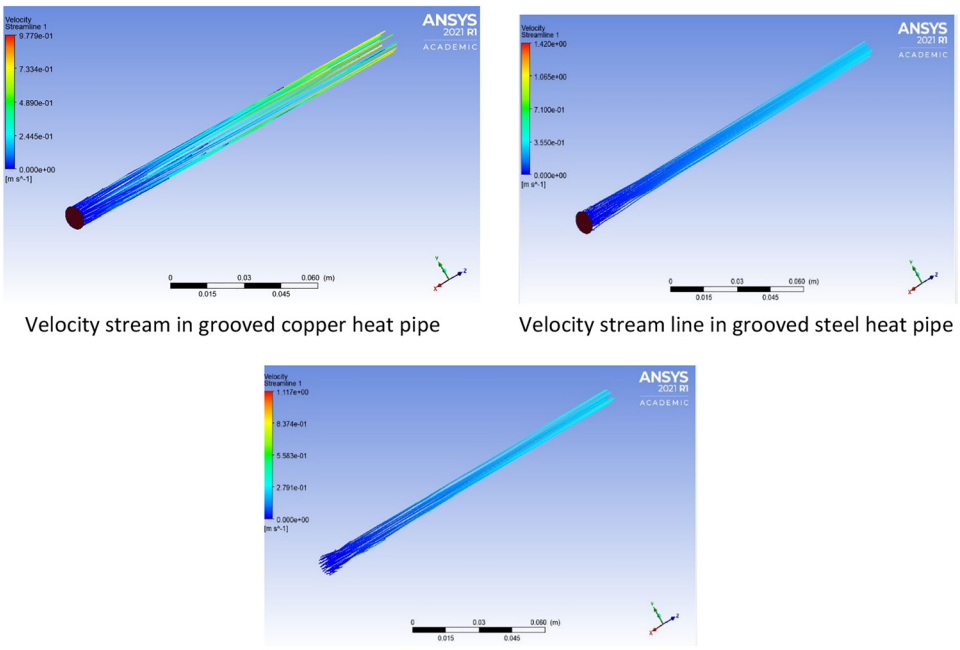

Fig. 9. Velocity stream in grooved heat pipe

condenser because of variations for a dry run. The slope of longitudinal temperature field rises as heat input increases, resulting in higher temperature swings throughout the condenser and evaporator sections, as seen in Fig. 12. A bigger temperature slope is necessary for increased heat transmission in simple conduction heat transfer. In comparison to another category, the copper-water combination HP has T_{max} at the evaporative section.

Figure 13 depicts the pressure variation in the symmetry plane of a real heat transfer tube. The pressure variations in

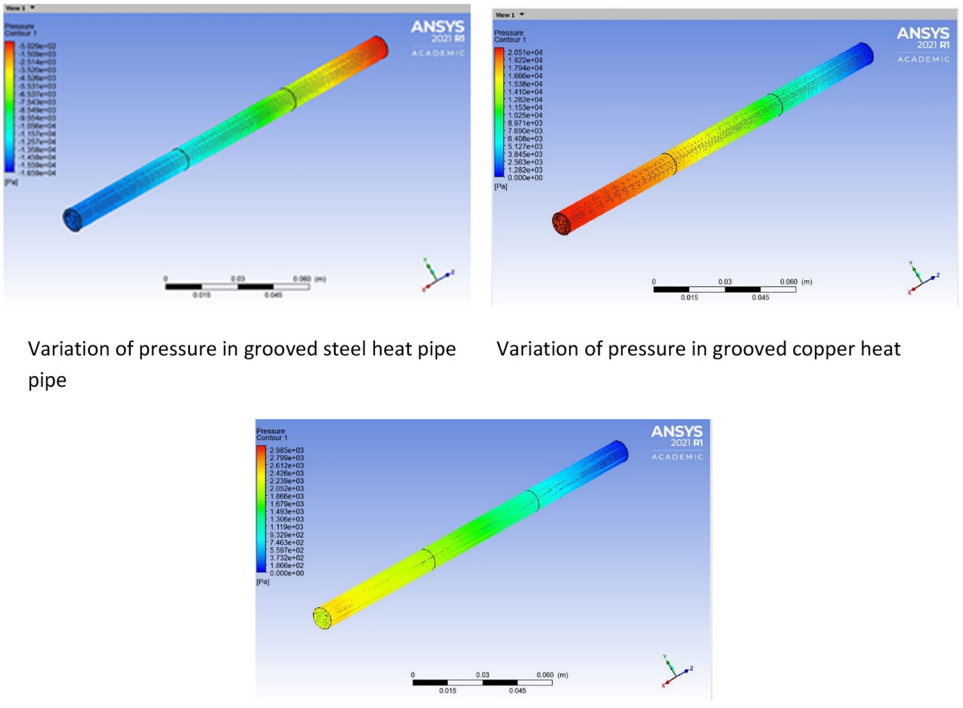

Fig. 10. Pressure variation in grooved heat pipe

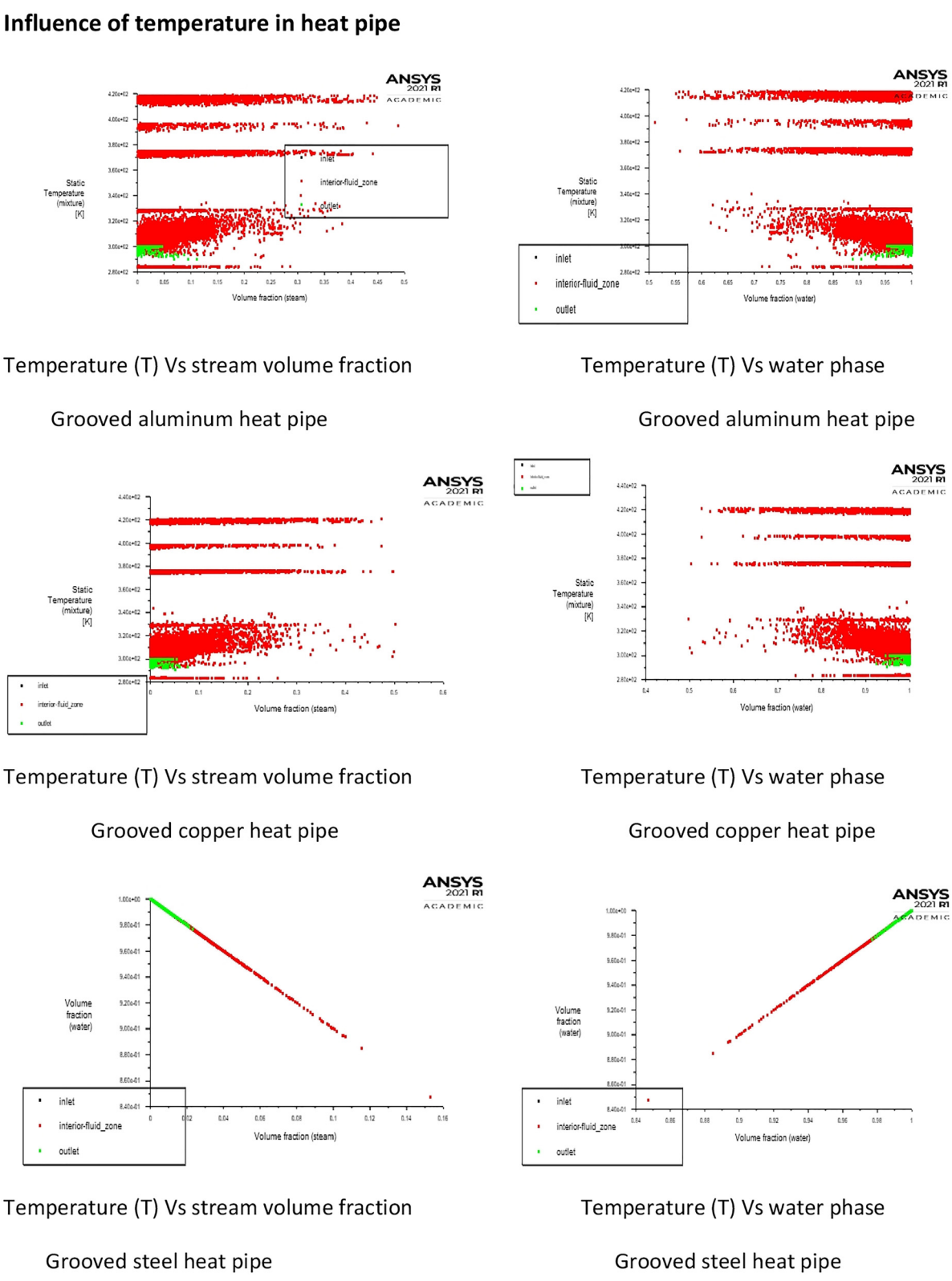

Fig. 11. Temperature variation with phase of base fluid

the non-grooved model are not nearly as similar as those in the grooved model, as seen in Fig. 13. As the pressure decreases, the dispersion becomes more uniform. Fluid losses grow as the actual heat pipe model includes condenser elements.

Figure 14 depicts the distribution of density drops inside a heat pipe. For the capillary force to push the vapour, the wick's capillary pressure must be greater than the pressure differential between the vapour and the liquid at the evaporator. The graph also shows that the liquid density lowers

Table 6. Parameter changes in grooved heat pipe

S. No	Parameter	Inlet	Evaporative section	Adiabatic section	Condenser section	Outlet
Water- steel	Temperature (K)	311	420.3	380.6	300	287
	Pressure (Pascal)	14,680	11,809	8,817	4,499	1,680
	Density (kg m^{-3})	996.2	888.6	889.2	979.2	988
	Velocity (m s^{-1})	0.1	1.488	1.784	2.17	2.24
	Turbulence (m^2 s^{-2})	0.057	0.15	0.513	0.724	0.799
Water -copper	Temperature (K)	309	421.1	391.6	322.7	312
	Pressure (Pascal)	14,640	16,620	15,100	6,042	1,510
	Density (kg m^{-3})	998.2	893.5	892.5	978.2	989
	Velocity (m s^{-1})	0.1	0.23	0.26	0.28	0.3
	Turbulence (m^2 s^{-2})	0.05	0.158	0.334	0.490	0.5
Water -aluminum	Temperature (K)	310	419.3	379.6	297	283
	Pressure (Pascal)	14,569	12,910	8,606	4,303	1,430
	Density (kg m^{-3})	998.2	898.5	898.5	998.2	999
	Velocity (m s^{-1})	0.1	1.267	1.934	2.04	2.3
	Turbulence (m^2 s^{-2})	0.06	0.12	0.468	0.689	0.8

Table 7. Parameter changes in conventional heat pipe

S. No.	Parameter	Inlet	Evaporative section	Adiabatic section	Condenser section	Outlet
Water- steel	Temperature (K)	309	370.3	330.54	297.4	305
	Pressure (Pascal)	14,545	10,450	9,679	9,760	9,853
	Density (kg m^{-3})	995.7	978.6	989.2	997.2	999.6
	Velocity (m s^{-1})	0.1	1.634	1.784	1.19	1.37
	Turbulence (m^2 s^{-2})	0.043	0.015	0.213	0.224	0.399
Water -copper	Temperature (K)	310	381.4	374.6	352.6	298
	Pressure (Pascal)	14,621	10,620	10,100	8,042	1,610
	Density (kg m^{-3})	997.8	894.3	894.3	988.7	989
	Velocity (m s^{-1})	0.1	1.73	1.88	1.99	2.10
	Turbulence (m^2 s^{-2})	0.053	0.158	0.189	0.246	0.364
Water -aluminum	Temperature (K)	309	382.4	368.6	317	288
	Pressure (Pascal)	14,550	10,913	9,706	5,103	1,253
	Density (kg m^{-3})	999.2	897.5	898.5	998.2	999
	Velocity (m s^{-1})	0.1	0.267	0.934	1.04	1.1
	Turbulence (m^2 s^{-2})	0.064	0.14	0.26	0.48	0.6

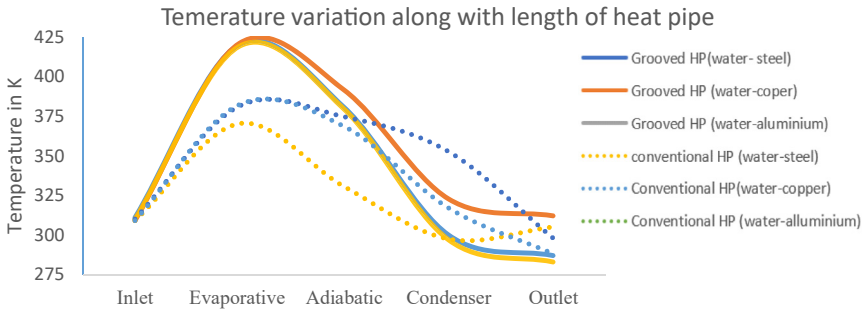

Fig. 12. Temperature variation Vs length of HP

higher when the heat pipe is operated against gravity. As a result, wick pumping and heat transfer are reduced. The degree of heat transfer reduction is determined by the heat pipe.

Figure 15 depicts the variation in HP's real heat transfer velocity. The exact velocity profile inside of an exact tube's outer tube is primarily the same as before the inside of a purely theoretical pipe's circular area, per this trend line; just one thing that is different is the motion scattering in the internal liquid; the impacts of grippy rubber give flow velocity into the inflatable raft, enhancing the rinsing impacts of the interior layer, and enhancing the heat transfer (Fig. 16).

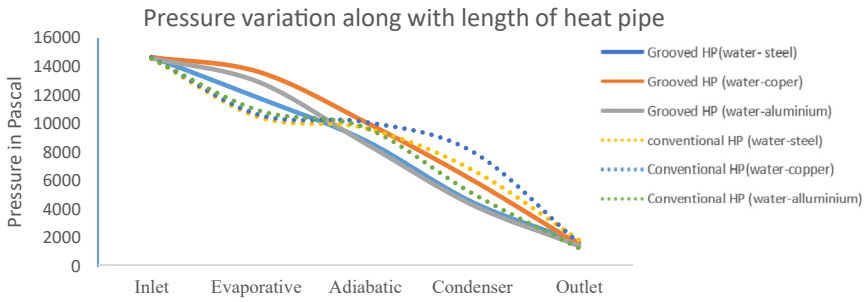

Fig. 13. Pressure variation Vs length of HP

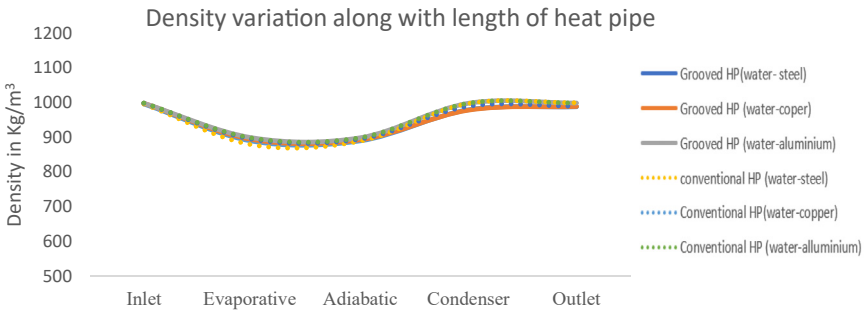

Fig. 14. Density variation Vs length of HP

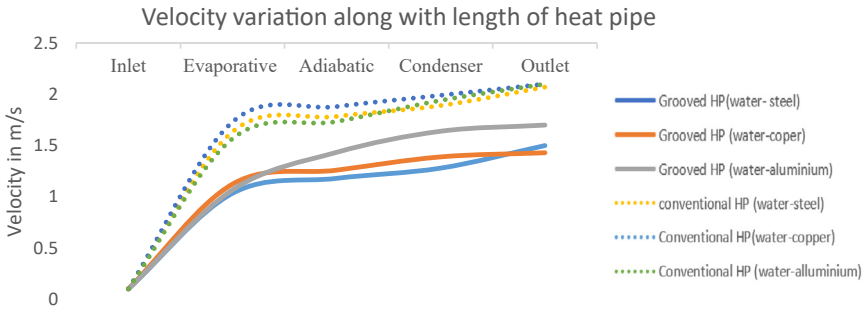

Fig. 15. Velocity variation Vs length of HP

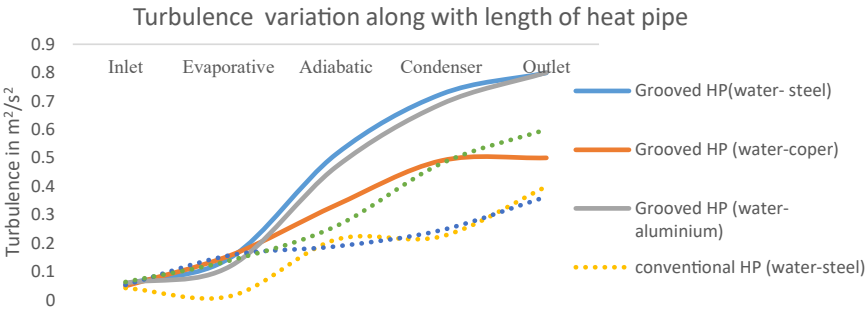

Fig. 16. Turbulence variation Vs length of HP

Because of the propped section, turbulence in grooved heat pipe is slightly higher than in regular heat pipe, resulting in flow limitation. There will be turbulence as a result. The outflow will have more turbulence due to the grooved section. In a conventional heat pipe, the line graph was plotted for aluminum, copper, and steel with their working circumstances. In a grooved heat pipe, the line graph was plotted for aluminum, copper, and steel with their working circumstances. As we can clearly see the difference between the conventional heat pipe and the grooved heat

pipe, we note that the maximum temperature values in the grooved heat pipe are noticeably greater than those in the conventional heat pipe when transmitting heat.

CONCLUSION

The effect of the groove, condensation and evaporation zone material, and cooling temperature on the homologous latent heat and nonlinear thermal of a twisted copper-water, aluminum-water, and steel-water heat pipe was critically examined. It was also investigated how heat and operation circumstances affect the immediate thermal characteristics of a twisty heat pipe. The crucial heat flow increases as the refrigeration temperature rises, but the heat transfer seen between chiller stays relatively consistent. Irrespectively of the chilling degree, the necessary heat flow skyrockets when the size of the exchanger is decreased in half. The crucial heat flux, on the other side, enhances noticeably as the evaporation planet warms above 50 °C. Greater roasting and chilling times enhance the comparable heat capacity. The rising length influences heat conductivity more than the precipitation area height. When heat is applied to a twisted wire heat pipe, the heats of the evaporate, isothermal, and condensing zones rise in order, after the warmth of the drying oven grows. The heat input is switched off, the twist heat pipe takes longer to recover to its original position than it does at start-up. Heat transfer is also efficient with copper-water combination heat pipes.

REFERENCES

[1] V. V. Cheverda, F. V. Ronshin, "Experimental study of heat transfers in a heat pipe," in *5th International Workshop on Heat/Mass Transfer Advances for Energy Conservation and Pollution Control*, August 13–16, 2019, https://doi.org/10.1088/1742-6596/1369/1/012053.

[2] S. Suman, R. Bandgar, D. Malage, P. Guja, A. Katkar, "Heat rejection application by using heat pipe," in *Proceedings of Conference on Advances on Trends in Engineering Projects (NCTEP-2019)*.

[3] H. Jouhara, A. Chauhan, T. Nannou, S. Almahmoud, B. Delpech, L.C. Wrobel, "Heat pipe based systems - advances and applications," Received 2 December, 10.1016, vol. 128, 1 June 2017, pp. 729–54.

[4] A. Shafieian, M. Khiadani, A. Nosrati, "Thermal performance of an evacuated tube heat pipe solar water heating system in cold season," Published by Elsevier Ltd. 2018, 10.1016, vol. 149, 25 February 2019, pp. 644–57.

[5] B. Delpech, M. Milani , L. Montorsi, D. Boscardin , A. Chauhan, S. Almahmoud, B. Axcell , H. Jouhara, "Energy efficiency enhancement and waste heat recovery in industrial processes by means of the heat pipe technology: case of the ceramic industry," Published by Elsevier Ltd. 2018, 10.1016, vol. 158, 1 September 2018, pp. 656–65.

[6] H. Fuke, S. Okazaki, H. Ogawa, Y. Miyazak, "Balloon flight demonstration of an oscillating heat pipe," 2020 World Scientific Publishing Co Pte Ltd, 10.1142, J. Astron. Inst., vol. 06, no. 02, 1740006, 2017.

[7] P. Ram Kumar, M. Sivasubramanian, P. RajeshKanna, P. Raveendiran, "Thermal characteristics analysis on multi- heat pipe induced heat exchanger," *Blue Eyes Intelligence Eng. Sci. Publ.* 2019, 10.35940.

[8] Z.Y. Jiang, Z.G. Qu, "Lithium–ion battery thermal management using heat pipe and phase change material during discharge–charge cycle: a comprehensive numerical study," 2019 Elsevier Ltd, 10.1016, vol. 242, 15 May 2019, pp. 378–92.

[9] M.M. Sarafraz, Z. Tian, I. Tlili, S. Kazi, M. Goodarzi, "Thermal evaluation of a heat pipe working with n-pentane-acetone and n-pentane-methanol binary mixtures," Published on 01 june 2019, 10.1007.

[10] H. Maddaha, M. Ghazvinib, M. Hossein Ahmadic, "Predicting the efficiency of CuO/water nanofluid in heat pipe heat exchanger using neural network," *Int. Commun. Heat Mass Transfer*, vol. 104, no. 2019, May 2019, pp. 33–40, 10.1016,Volume 104.

[11] A. Shafieian, M. Khiadani, A. Nosrati, "Strategies to improve the thermal performance of heat pipe solar collectors in solar systems," *Energ. Convers. Manag.*, vol. 183, no. 2019, 1 March 2019, pp. 307–31, 10.1016.

[12] A. Wei, J. Qu, H. Qiu, C. Wang, G. Cao, "Heat transfer characteristics of plug-in oscillating heat pipe with binary-fluid mixtures for electric vehicle battery thermal management," *Int. J. Heat Mass Transfer.*, vol. 135, no. 2019, June 2019, pp. 746–60, 10.1016.

[13] T.M.O. Diallo, M. Yu, J. Zhou, X. Zhao, S. Shittu, G. Li, J. Ji, D. Hardy, "Energy performance analysis of a novel solar PVT loop heat pipe employing a microchannel heat pipe evaporator and a PCM triple heat exchanger," vol. 167, 15 January 2019, pp. 866–88, Published on 2018, 10.1016.

[14] A. Sözena, M. Gürüb, A. Khanlaric, E. Çiftçia, "Experimental and numerical study on enhancement of heat transfer characteristics of a heat pipe utilizing aqueous clinoptilolite nanofluid," Available online 21 June 2019,10.1016, Vol. 160, September 2019, 114001.

[15] J. Qua, Q. Sun, H. Wang, D. Zhang, J. Yuan, "Performance characteristics of flat-plate oscillating heat pipe with porous metal-foam wicks," 2019 Elsevier Ltd, 10.1016, vol. 137, July 2019, pp. 20–30.

[16] Q. Su, S. Chang, M. Song , Y. Zhao, C. Dang, "An experimental study on the heat transfer performance of a loop heat pipe system with ethanol-water mixture as working fluid for aircraft anti-icing," Available online from 11 May 2019,10.1016, vol. 139, August 2019, pp. 280–92.

[17] G Chena, Y. Tanga, Z. Wana, G. Zhonga, H. Tanga, J. Zeng, "Heat transfer characteristic of an ultra-thin flat plate heat pipe with surface functional wicks for cooling electronics," 2018 Elsevier Ltd,10.1016, vol. 100, January 2019, pp. 12–9.

[18] Y.H. Diaoa, L. Lianga, Y.H. Zhaoa, Z.Y. Wanga, F.W. Baib, "Numerical investigation of the thermal performance enhancement of latent heat thermal energy storage using longitudinal rectangular fins and flat micro-heat pipe arrays," 2018 Elsevier Ltd, 10.1016, vols 233–234, 1 January 2019, pp. 894–905.

[19] S. Miao, J. Sui, Y. Zhang, F. Yao, X. Liu, "Experimental study on thermal performance of a bent copper-water heat pipe," Published 30 June 2020, 10.1155.

[20] J. Song, Y. Bi, S. Liu, G. Zhong, C. Wang, J. Wang, S. Song, "An experimental and engineering application of an active snow-melting

system for highways based on heat-pipe technology," IOP Publishing on 2019, 10.1088.

[21] S.V. Channapattana, S.B. Raut, A.A. Pawar, S. Campli, S.S. Sarnobat, T. Dey, "Heat transfer performance analysis of screen mesh wick heat pipe using CuO nano fluid," Published on March 3, 2019,10.1055, vols 233–234, 1 January 2019, pp. 894–905.

[22] M. Shafiey Dehaja, M.Z. Mohiabadi, "Experimental investigation of heat pipe solar collector using MgO nanofluids," Published on 2018 by Elsevier B.V, 10.1016, vol. 191, March 2019, pp. 91–9.

[23] S. Shittu, G. Li, X. Zhao, Y.G. Akhlaghi, X. Ma, M. Yu, "Comparative study of a concentrated photovoltaic-thermoelectric system with and without flat plate heat pipe," Published on 2019 by Elsevier Ltd,10.1016, vol. 193, 1 August 2019, pp. 1–14.

[24] M.M. Sarafraz, O. Pourmehran, B. Yang, M. Arjomandi, "Assessment of the thermal performance of a thermosyphon heat pipe using zirconia-acetone nanofluids," Published online on 19 January 2019,10.1016, vol. 136, June 2019, pp. 884–95.

[25] M. Kaya, A.E. Gurel, U. Agbulut, İ. Ceylan, S. Çelik, A. Ergün, B. Acar, "Performance analysis of using CuO-Methanol nanofluid in a hybrid system with concentrated air collector and vacuum tube heat pipe," Published online on 22 August 2019, 10.1016, vol. 199, 1 November 2019, 111936.

[26] A. Wei, J. Qu, H. Qiu, C. Wang, G. Cao, "Heat transfer characteristics of plug-in oscillating heat pipe with binary-fluid mixtures for electric vehicle battery thermal management," *Int. J. Heat Mass Transfer*, vol. 135, June 2019, pp. 746–60, 2019,10.1016.